

## Error threshold in finite populations

D. Alves and J. F. Fontanari  
Instituto de Física de São Carlos  
Universidade de São Paulo  
Caixa Postal 369  
13560-970 São Carlos SP  
Brazil

We extend the deterministic population genetics formulation of the quasispecies model [Phys. Rev. E **54**, 4048 (1996)] to finite populations in order to investigate analytically the dependence of the error threshold on the population size. In particular, we find that for large populations the replication accuracy at the threshold increases linearly with the reciprocal of the population size. Moreover, in contrast to the deterministic case, for small populations the error threshold transition is inevitable, whatever the value of the selective advantage of the master string.

An important issue in the investigation of the dynamics of competing self-reproducing macromolecules, whose paradigm is Eigen's quasispecies model [1], is the effect of the finite size of the population on the error threshold phenomenon that limits the length of the molecules [2]. The quasispecies model was originally formulated as a deterministic kinetic theory described by a set of ordinary differential equations for the concentrations of the different types of molecules that compose the population. Such formulation, however, is valid only in the limit where the total number of molecules  $N$  goes to infinity. More pointedly, in this model a molecule is represented by a string of  $\nu$  digits  $(s_1, s_2, \dots, s_\nu)$ , with the variables  $s_\alpha$  allowed to take on  $\kappa$  different values, each of which representing a different type of monomer used to build the molecule. For sake of simplicity, in this paper we will consider only binary strings, i.e.,  $s_\alpha = 0, 1$ . The concentrations  $x_i$  of molecules of type  $i = 1, 2, \dots, 2^\nu$  evolve in time according to the following differential equations [1, 2]

$$\frac{dx_i}{dt} = \sum_j W_{ij} x_j - [D_i + \Phi(t)] x_i, \quad (1)$$

where the constants  $D_i$  stand for the death probability of molecules of type  $i$ , and  $\Phi(t)$  is a dilution flux that keeps the total concentration constant. This flux introduces a nonlinearity in (1), and is determined by the condition  $\sum_i dx_i/dt = 0$ . The elements of the replication matrix  $W_{ij}$  depend on the replication rate or fitness  $A_i$  of the molecules of type  $i$  as well as on the Hamming distance  $d(i, j)$  between strings  $i$  and  $j$ . They are given by

$$W_{ii} = A_i q^\nu \quad (2)$$

and

$$W_{ij} = A_i q^{\nu-d(i,j)} (1-q)^{d(i,j)} \quad i \neq j, \quad (3)$$

where  $0 \leq q \leq 1$  is the single-digit replication accuracy, which is assumed to be the same for all digits. Henceforth we will set  $D_i = 0$  for all  $i$ . The quasispecies concept is illustrated more neatly for the single-sharp-peak replication landscape, in which we ascribe the replication rate  $a > 1$  to the so-called master string  $(1, 1, \dots, 1)$ , and the replication rate 1 to the remaining strings. In this context, the parameter  $a$  is termed selective advantage of the master string. As the error rate  $1 - q$  increases, two distinct regimes are observed in the population composition: the *quasispecies* regime characterized by the master string and its close neighbors, and the *uniform* regime where the  $2^\nu$  strings appear in the same proportion. The transition between these regimes takes place at the error threshold  $1 - q_t$ , whose value depends on the parameters  $\nu$  and  $a$  [1, 2]. A genuine thermodynamic order-disorder phase transition occurs in the limit  $\nu \rightarrow \infty$  only [3, 4, 5].

To take into account the effect of finite  $N$ , the deterministic kinetic formulation was replaced by a stochastic formulation based on a master equation for the probability distribution of the number of different types of molecules in the population [6, 7]. However, the extreme approximations employed to derive results from

that master equation or from related Langevin equations [8, 9] have hindered the analysis of the error threshold for finite populations. An alternative approach to study stochastic chemical reaction networks is the algorithm proposed by Gillespie [10], which has been successfully employed to simulate numerically the quasispecies model, providing thus a base line for analytical investigations [11].

Recently, a population genetics formulation of the deterministic quasispecies model has been proposed that, for a certain class of replication landscapes, yields results that are qualitatively similar to those obtained by solving the kinetic equations [12]. That approach is based on the following two simplifying assumptions. First, it is assumed that the molecules are characterized solely by the number of monomers 1 they have, regardless of the particular positions of these monomers inside the molecules. Hence there are only  $\nu + 1$  different types of molecules which are labeled by the integer  $P = 0, 1, \dots, \nu$ . This assumption is not so far-fetched since the feature that distinguishes the molecules is their replication rates  $A_i$ , which in most analyses has been chosen to depend on  $P$  only, i.e.,  $A_i = A_P$  [2]. In this work we will consider the single-sharp-peak replication landscape, which clearly satisfies that condition. Second, denoting the frequency of monomers 1 in generation  $t$  by  $p_t$ , it is assumed that the molecule frequencies are given by the binomial distribution

$$\Pi_P = \binom{\nu}{P} (p_t)^P (1 - p_t)^{\nu - P}, \quad (4)$$

where we have omitted the generation index  $t$  in  $\Pi_P$ . Thus, in each generation the monomers are sampled with replacement from a pool containing monomers 1 and 0 in the proportions  $p_t$  and  $1 - p_t$ , respectively. In other words, the population composed of the offspring of the molecules present in the generation  $t - 1$  is destroyed and its monomer frequency  $p_t$  used to create an entire new population according to (4). Although this procedure destroys the correlations between the molecules, it does not cause any significant loss of genetic information since the fitness of the molecules depend only on the number of monomers 1 they have, which, in the average, is not affected by the procedure. This is probably the reason why, despite this drastic assumption, the population genetics formulation is so effective in describing the qualitative features of the quasispecies model. With these assumptions a simple recursion relation for the monomer frequency  $p_t$  can be readily derived [12].

The goal of this work is to extend the population genetics formulation to investigate the evolution of finite populations. More specifically, since for finite  $N$  the monomer frequency  $p_t$  is a random variable, we will derive a recursion relation for its average value  $\bar{p}_t$ . We will concentrate mainly on the dependence of the error threshold on the population size  $N$ .

In each generation the population is described by the vector  $\mathbf{n} = (n_0, \dots, n_\nu)$  where  $n_P$  is the number of molecules of type  $P$ , so that  $\sum_P n_P = N$ . Similarly to the deterministic case, we have to resort to a rather arbitrary assumption to relate the molecule frequencies  $\Pi_P$  to the vector  $\mathbf{n}$ . In particular, we consider a molecule pool containing the different molecule types in the proportions  $\Pi_P$ , so that  $\mathbf{n}$  is

distributed by the multinomial distribution

$$\mathcal{P}(\mathbf{n}) = \frac{N!}{n_0! n_1! \dots n_\nu!} \Pi_0^{n_0} \Pi_1^{n_1} \dots \Pi_\nu^{n_\nu}. \quad (5)$$

As before, in each generation the molecules are sampled with replacement from the molecule pool. The changes in the population composition  $\mathbf{n}$  are due to the driving of natural selection, modeled by the replication rate  $A_P$ , and to mutations, modeled by the error rate per digit  $1 - q$ . Following the prescription used in the implementation of the standard genetic algorithm [13], we consider first the effect of natural selection and then the effect of mutations. As usual we assume that the number of offspring that each molecule contributes to the new generation is proportional to its relative replication rate which, for molecules of type  $P$ , is defined by

$$W_P(\mathbf{n}) = \frac{n_P A_P}{\sum_R n_R A_R}. \quad (6)$$

Thus the population composition after selection is described by the random vector  $\mathbf{n}' = (n'_0, \dots, n'_\nu)$  which is distributed according to the conditional probability distribution

$$\mathcal{P}_s(\mathbf{n}' | \mathbf{n}) = \frac{N!}{n'_0! n'_1! \dots n'_\nu!} [W_0(\mathbf{n})]^{n'_0} [W_1(\mathbf{n})]^{n'_1} \dots [W_\nu(\mathbf{n})]^{n'_\nu}. \quad (7)$$

Next we consider the changes in  $\mathbf{n}'$  due to mutations. After mutation, the population is described by  $\mathbf{n}'' = (n''_0, \dots, n''_\nu)$  whose components are written as

$$n''_P = \sum_{R=0}^{\nu} n''_{PR}, \quad (8)$$

where the integer  $n''_{PR}$  stands for the number of molecules of type  $R$  that have mutated to a molecule of type  $P$ . Clearly,  $n'_R = \sum_P n''_{PR}$ . We note that the probability of mutation from a molecule of type  $R$  to a molecule of type  $P$  is given by [14]

$$M_{PR} = \sum_{Q=Q_l}^{Q_u} \binom{R}{Q} \binom{\nu - R}{P - Q} q^{\nu - P - R + 2Q} (1 - q)^{P + R - 2Q}, \quad (9)$$

where  $Q_l = \max(0, P + R - \nu)$  and  $Q_u = \min(P, R)$ . The population is more conveniently described by the set  $\{n''_{PR}\}$  rather than by  $\mathbf{n}''$ . In fact, given  $n'_R$  the conditional probability distribution of  $\{n''_{PR}\}$  is again a multinomial

$$\mathcal{P}_m(n''_{0R}, n''_{1R}, \dots, n''_{\nu R} | n'_R) = \frac{n'_R!}{n''_{0R}! n''_{1R}! \dots n''_{\nu R}!} M_{0R}^{n''_{0R}} M_{1R}^{n''_{1R}} \dots M_{\nu R}^{n''_{\nu R}} \quad (10)$$

for  $R = 0, \dots, \nu$ . In this framework the frequency of monomers 1 in the next generation  $p_{t+1}$  is given simply by  $\frac{1}{N\nu} \sum_R \sum_P P n''_{PR}$ . This frequency is used to generate

the new population of  $N$  molecules of length  $\nu$  according to the distributions (4) and (5). The procedure is then repeated again. In figure 1 we present the results of the simulations for the single-sharp-peak replication landscape. The initial population is set with  $p_0 = 1$  and left to evolve for  $2 \cdot 10^4$  generations. No significant differences were found for longer runs or for different choices of the initial frequency  $p_0$ . Each data point involves two kinds of average: for each run we average over the monomer frequencies in the last 100 generations; this value is then averaged over 100 runs. We note that even if the populations are identical in the initial generation, the random character of the transitions  $\mathbf{n} \rightarrow \mathbf{n}' \rightarrow \mathbf{n}''$  will make them distinct in the next generation.

To derive an analytical recursion relation for  $\bar{p}_t$  we consider the following approximate procedure that greatly facilitates the analysis: instead of averaging over the populations only after the stationary regime is reached, we perform this average in each generation. The result obtained  $\bar{p}_t$  is then used to build the new populations. Of course, in doing so we neglect the fluctuations of  $p_t$  for the different runs. Within this framework the average frequency of monomers 1 in generation  $t + 1$  is written as

$$\bar{p}_{t+1} = \frac{1}{N\nu} \sum_{\mathbf{n}} \sum_{\mathbf{n}'} \mathcal{T}_m(\mathbf{n}') \mathcal{P}_s(\mathbf{n}' | \mathbf{n}) \mathcal{P}(\mathbf{n}) \quad (11)$$

where

$$\mathcal{T}_m(\mathbf{n}') = \sum_{\{n''_{PR}\}} \sum_R \sum_P P n''_{PR} \mathcal{P}_m(\{n''_{PR}\} | \mathbf{n}'). \quad (12)$$

The summations over  $\{n''_{PR}\}$  and  $P$  can be easily carried out and yield

$$\begin{aligned} \mathcal{T}_m(\mathbf{n}') &= \sum_R \sum_P P M_{PR} n'_R \\ &= \sum_R [qR + (1-q)(\nu - R)] n'_R. \end{aligned} \quad (13)$$

Moreover, using  $\sum_{n'_R} n'_R \mathcal{P}_s(\mathbf{n}' | \mathbf{n}) = N W_R(\mathbf{n})$  we rewrite (11) as

$$\bar{p}_{t+1} = \frac{1}{\nu} \sum_{\mathbf{n}} \sum_R [qR + (1-q)(\nu - R)] W_R(\mathbf{n}) \mathcal{P}(\mathbf{n}). \quad (14)$$

To proceed further we must specify the replication rate  $A_P$ . In the case of the single-sharp-peak replication landscape, i.e.,  $A_\nu = a$  and  $A_P = 1$  for  $P \neq \nu$ , the summations over  $n_0, \dots, n_{\nu-1}$  as well as over  $R$  can be readily carried out. The final result is

$$\bar{p}_{t+1} = 1 - q + (2q - 1) \left[ \bar{p}_t^{\nu N} + \sum_{n=0}^{N-1} B_n \frac{\bar{p}_t - \bar{p}_t' + \frac{r}{1-r} a (1 - \bar{p}_t')}{1 + r(a - 1)} \right], \quad (15)$$

where

$$B_n = \binom{N-1}{n} (\bar{p}_t')^n (1 - \bar{p}_t')^{N-1-n}, \quad (16)$$

and  $r = n/N$ . Here we have set  $n_\nu = n$ . For  $N \rightarrow \infty$  the sum is dominated by the closest integer to  $(N-1)\bar{p}_t^\nu$ , so that  $r \rightarrow \bar{p}_t^\nu$  and the recursion relation for the deterministic case is recovered [12].

For the parameters of figure 1, the analysis of the fixed points of Eq. (15) indicates that for small error rates there is only one stable fixed point  $\bar{p}^* \approx 1$ , which we associate to the quasispecies regime. As  $1-q$  increases, a second stable fixed point  $\bar{p}^* \approx 0.5$  appears. This fixed point, which is associated to the uniform regime, has the largest basin of attraction. The two stable fixed points coexist and compete until the error rate reaches the threshold value  $1-q_t$ , at which the quasispecies fixed point disappears discontinuously. In the coexistence region the steady-state frequency  $\bar{p}_\infty$  depends on the value of  $\bar{p}_0$ . This behavior pattern is illustrated in figure 1, where we present  $\bar{p}_\infty$  for two different initial frequencies,  $\bar{p}_0 = 1$  (solid curve) and  $\bar{p}_0 = 0.7$  (dashed curve). The agreement between the results of the simulations, which do not depend on  $p_0$ , and the analytical approximation for  $\bar{p}_0 = 0.7$  is very good already for  $N = 50$ . This indicates that the effect of the fluctuations neglected in our analytical approximation is to eliminate the region of coexistence of the fixed points, and that the unique steady-state can be well characterized by the fixed point with the largest basin of attraction. We note that in the simulations of the finite  $N$  quasispecies model the location of the error threshold is determined by the inflection point of the smooth curve that interpolates the numerical data [11].

Similarly to the deterministic case, for fixed  $\nu$  and not too small  $N$ , the size of the jump in  $\bar{p}_\infty$  at the error threshold decreases as the selective advantage  $a$  increases, and disappears altogether at a critical point  $1-q_c$  [12]. For fixed  $a$ , the jump size decreases with increasing  $N$  and, for small values of  $\nu$ , may even disappear for large enough  $N$ . In figure 2 we show the replication accuracy at the threshold  $q_t$  as a function of the reciprocal of the population size. We use  $q_t$  instead of  $1-q_t$  to facilitate the comparison with the results obtained using Gillespie's algorithm and other analytical approximations for the finite  $N$  quasispecies model (see Figure 30 of [2], for instance). In fact, there is a good qualitative agreement between these results. For sake of consistency with previous work [12], we have defined  $1-q_t$  as the error rate at which the quasispecies fixed point disappears, although our simulations suggest that it should be defined as the error rate at which the uniform fixed point appears. However, there is no qualitative differences between the behavior patterns of these error rates as the control parameters vary and, in particular, the location of the critical points are the same for both cases. The increase of  $q_t$  with decreasing  $N$  is expected since the fluctuations become stronger for small  $N$  and so, the replication must be more accurate in order to keep the master string in the population. In particular, for large  $N$  we find that  $q_t$  increases linearly with  $1/N$ . The empty circles in figure 2 indicate the location of the critical points that appear for  $\nu = 7, 8$ , and 9. For  $\nu \leq 5$ , as well as for  $q < q_c$ , there is no error threshold transition. In figure 3 we show the size dependence of the critical error rate  $1-q_c$  for fixed  $\nu$ . We note that the selective advantage parameter varies over these curves, assuming the critical value  $a_c(\nu, N)$ . The filled

circles indicate the reciprocal population size beyond which there is always an error threshold transition, whatever the value of the selective advantage  $a$ . This contrasts to the deterministic case, where it was always possible to avoid the error threshold catastrophe by choosing  $a$  sufficiently large [12].

Finally, we should mention that by focusing on the evolution of the average molecule frequencies  $\bar{\Pi}_P$  ( $P = 0, \dots, \nu$ ) rather than on the average monomer frequency  $\bar{p}$  we could dispense with assumption (4), so that our approach would rely on only one arbitrary assumption, namely, Eq. (5). However, the convenience of describing the population evolution through a single parameter was a weighty argument in favor of using (4) as well. Yet even then we had to resort to an approximation, akin to the annealed approximation of the statistical mechanics of disordered systems, to derive an analytical recursion relation for  $\bar{p}_t$ .

**Acknowledgments** This work was supported in part by Conselho Nacional de Desenvolvimento Científico e Tecnológico (CNPq).

## References

- [1] M. Eigen, *Naturwissenschaften* **58**, 465 (1971).
- [2] M. Eigen, J. McCaskill and P. Schuster, *Adv. Chem. Phys.* **75**, 149 (1989).
- [3] I. Leuthäusser, *J. Chem. Phys.* **84**, 1884 (1986); *J. Stat. Phys.* **48**, 343 (1987).
- [4] P. Tarazona, *Phys. Rev. A* **45**, 6038 (1992).
- [5] S. Galluccio, R. Graber and Y-C. Zhang, *J. Phys. A* **29**, L249 (1996).
- [6] W. Ebeling and R. Feistel, *Ann. Physik* **34**, 81 (1977).
- [7] J. S. McCaskill, *Biol. Cybern.* **50**, 63 (1984).
- [8] H. Inagaki, *Bull. Math. Biol.* **44**, 17 (1982).
- [9] Y-C. Zhang, *Phys. Rev. E* **55**, R3817 (1997).
- [10] D. Gillespie, *J. Comp. Phys.* **22**, 403 (1976); *J. Phys. Chem.* **81**, 2340 (1977).
- [11] M. Novak and P. Schuster, *J. Theor. Biol.* **137**, 375 (1989).
- [12] D. Alves and J. F. Fontanari, *Phys. Rev. E* **54**, 4048 (1996).
- [13] D. E. Goldberg, *Genetic Algorithms in Search, Optimization and Machine Learning* (Addison-Wesley, Reading, 1989).
- [14] G. Woodcock and P. G. Higgs, *J. Theor. Biol.* **179**, 61 (1996)

## Figure captions

**Fig. 1** Average steady-state frequency of monomers 1 as a function of the error rate per digit for  $N = 5$  ( $\circ$ ),  $N = 50$  ( $\square$ ) and  $N = 500$  ( $\triangle$ ). The theoretical predictions for  $\bar{p}_0 = 1$  and  $\bar{p}_0 = 0.7$  are given by the solid and dashed curves, respectively. The parameters are  $\nu = 10$  and  $a = 10$ .

**Fig. 2** Replication accuracy at the error threshold as a function of the reciprocal of the population size for  $a = 30$  and (from bottom to top)  $\nu = 7$  to  $\nu = 20$ . For  $\nu \leq 9$  the transition lines terminate at critical points (empty circles).

**Fig. 3** Error rate at the critical point as a function of the reciprocal of the population size for (from bottom to top)  $\nu = 6$  to  $\nu = 10$ . The filled circles indicate the values of  $N$  below which the error threshold transition always occurs.

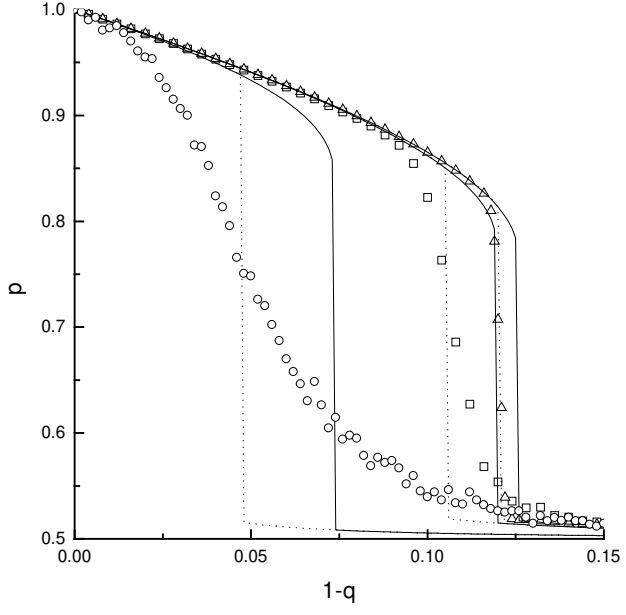


Figure 1



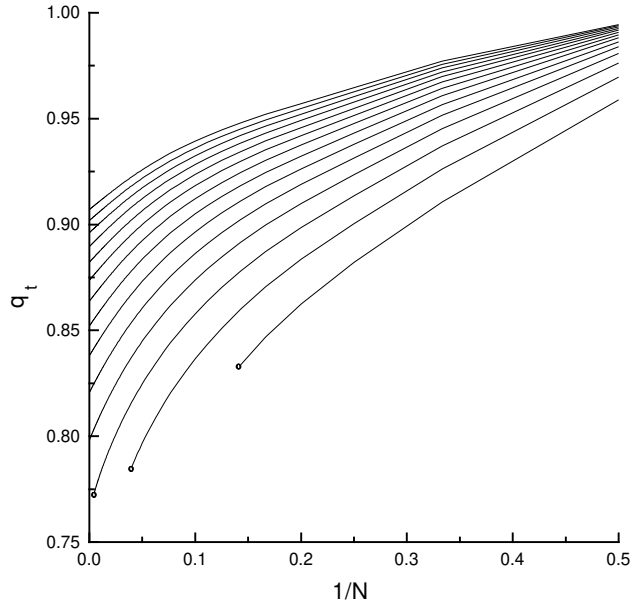


Figure 2



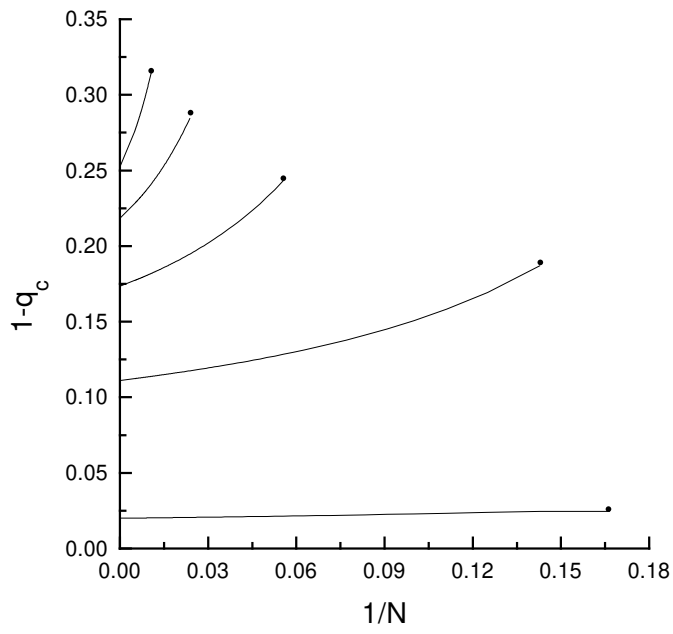


Figure 3

